PRESUPERNOVA EVOLUTION AND NUCLEOSYNTHESIS OF ROTATING MASSIVE STARS @ VARIOUS METALLICITIES

Marco Limongi

INAF – Osservatorio Astronomico di Roma, ITALY

Kavli IPMU, University of Tokyo, JAPAN

marco.limongi@oa-roma.inaf.it

and

Alessandro Chieffi

INAF – Istituto di Astrofisica e Planetologia Spaziali, Italy

CSPA, Monash Univesity, Australia

alessandro.chieffi@iasf-roma.inaf.it

PRIN MIUR 2010-2011, project "The Chemical and dynamical Evolution of the Milky Way and Local Group Galaxies". PI: F. Matteucci

PRESUPERNOVA EVOLUTIONS

INITIAL MASSES: 13, 15, 20, 25, 30, 40, 60, and 80 $M_\odot$

INITIAL COMPOSITIONS:

[Fe/H]=0, Z=1.345 10^{-2}	Asplund et al. 2009
[Fe/H]=-1, Z=3.236 10^{-3}	Scaled solar $Fe/Fe_\odot$=0.1,0.01,0001
[Fe/H]=-2, Z=3.236 10^{-4}	except
[Fe/H]=-3, Z=3.236 10^{-5}	[C/Fe]=0.18
	[O/Fe]=0.47
	[Mg/Fe]=0.27
	[Si/Fe]=0.37
	[S/Fe]=0.35
	[Ar/Fe]=0.35
	[Ca/Fe]=0.33
	[Ti/Fe]=0.23
	(Cayrel+ 2004 and Spite+ 2005)

INITIAL EQUATORIAL VELOCITIES: 0, 150, 300 km/s

PRESUPERNOVA EVOLUTIONS

All models computed with the FRANEC (Frascati RAphson Newton Evolutionary Code) 6.0

Major improvements compared to the release 4.0 (ML & Chieffi 2003) and 5.0 (ML & Chieffi 2006)

- FULL COUPLING of: Physical Structure - Nuclear Burning - Chemical Mixing (convection, semiconvection, rotation)

- INCLUSION OF ROTATION:
  - Shellular Rotation (Meynet & Maeder 1997)
  - Transport of Angular Momentum due to shear instabilities and meridional circulation (Advection/Diffusion equation, Meynet & Maeder 2000)
  - Coupling of Rotation and Mass Loss (angular momentum losses due to stellar wind and mechanical mass losses due to rotation)

- MASS LOSS:
  - OB: Vink et al. 2000,2001
  - RSG: de Jager 1988+Van Loon 2005 (Dust driven wind)
  - WR: Nugis & Lamers 2000
  - Supra Eddington Mass Loss
  - Mechanical mass loss due to rotation (close to critical velocity)

PRESUPERNOVA EVOLUTIONS

$$\frac{\partial P}{\partial M} = -\frac{GM}{4\pi R^4} f_P$$

$$\frac{\partial R}{\partial M} = \frac{1}{4\pi \rho R^2}$$

$$\frac{\partial T}{\partial M} = -\frac{GMT}{4\pi R^2 P} \nabla \frac{f_T}{f_P}$$

$$\frac{\partial L}{\partial M} = \varepsilon$$

$$\frac{\partial Y_i}{\partial t} = \left(\frac{\partial Y_i}{\partial t}\right)_{\rm nuc} + \frac{\partial}{\partial m}\left[\left(4\pi \rho r^2\right)^2 \left(D_{\rm mix} + D_{\rm semi} + D_{\rm rot}\right)\left(\frac{\partial X_i}{\partial m}\right)\right]$$

FRANEC 6.0: Numerical Scheme

FULL COUPLING and simultaneous solution of: Physical Structure - Nuclear Burning - Chemical Mixing (convection, semiconvection, rotation) equations

$$\rho \frac{d}{dt}\left(r^2 \omega\right) = \frac{1}{5r^2}\frac{\partial}{\partial r}\left(\rho r^4 \omega U\right) + \frac{1}{r^2}\frac{\partial}{\partial r}\left(\rho D_{\rm shear} r^4 \frac{\partial \omega}{\partial r}\right)$$

Meridional Circulation — Shear Instabilities

(4^{th} order → 4 ODE solved by means of a relaxation method)

(Chieffi & Limongi 2013, ApJ, 764, 21)

PRESUPERNOVA EVOLUTIONS

FRANEC 6.0: NUCLEAR NETWORK

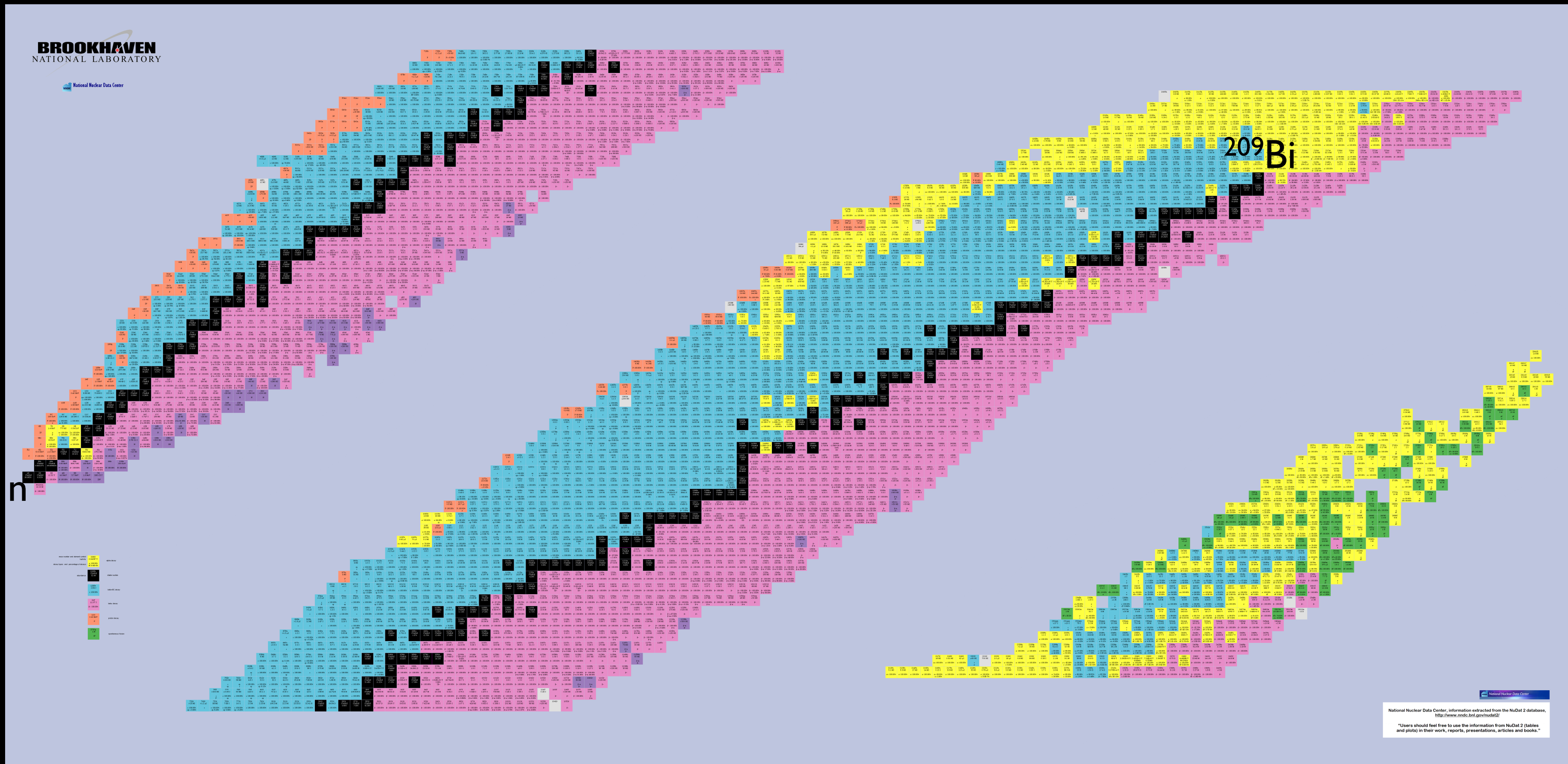

- TWO NUCLEAR NETWORKS FULLY COUPLED TO THE EVOLUTION:
  - 200 isotopes from n to ^{209}Bi (500 reactions) H/He Burning
  - 320 isotopes from n to ^{209}Bi (3000 reactions) Advanced Burning

CALIBRATION OF THE ROTATIONAL MIXING EFFICIENCY

All the uncertainties in the treatment of rotation may be accounted for essentially by means of two free parameters

f_c that multiplies the diffusion coefficient adopted for the mixing of the chemicals

$$D = f_c D_{\rm rot} = f_c \left(D_{\rm shear} + D_{\rm mc} \right)$$

f_μ that multiplies the gradient of molecular weight $\nabla_\mu \rightarrow f_\mu \nabla_\mu$ (Heger+ 2000)

f_c, f_μ calibrated in order to reproduce the observed nitrogen surface abundances as a function of the projected rotational velocity for stars in the LMC sample (NGC 2004) of the FLAMES survey (Hunter+ 2009)

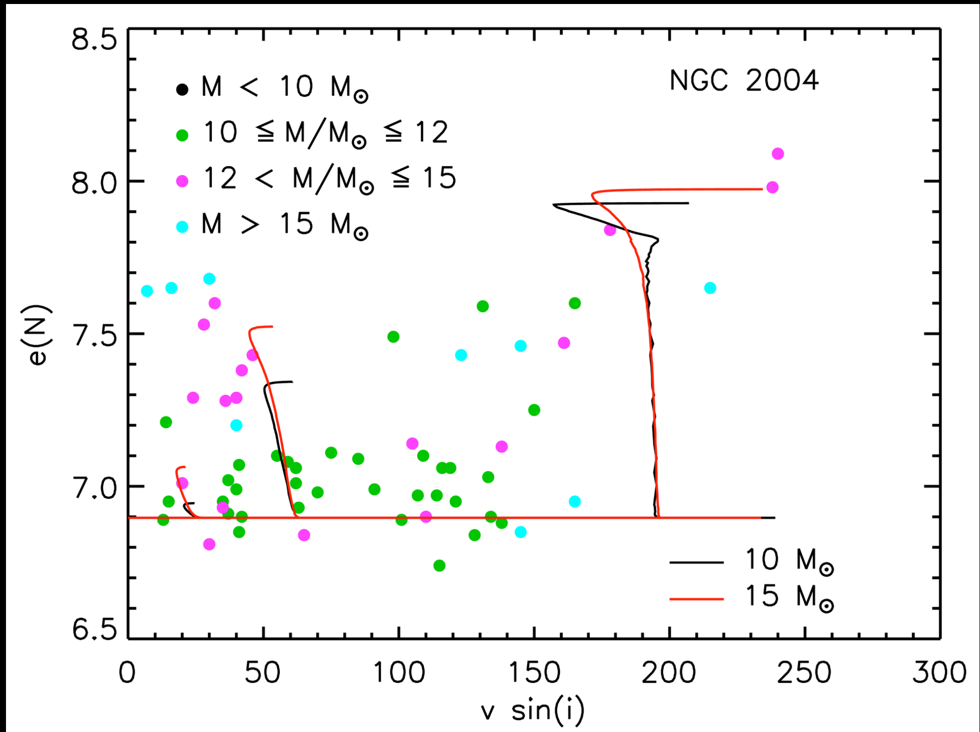

DIRECT EFFECTS

Internal Mixing (meridional circulation, shear diffusion)

- Larger Cores and Longer Evolutionary Times (these effects are negligible after core He depletion due to the dramatic shortening of the advanced evolutionary phases)
- Surface enrichment in elements produced in the innermost zones
- More Compact Structures → Higher Luminosities

Reduction of the Effective Gravity
(centrifugal force, angular momentum transport)

- More Expanded Envelopes → Lower Effective Temperatures

Mechanical Mass Loss

- Increase of Mass Loss if the star reaches the Critical Velocity

INDIRECT EFFECTS

Higher Luminosities and Lower Effective Temperatures → Increase of Mass Loss efficiency

He Core Mass @ Core H Depletion

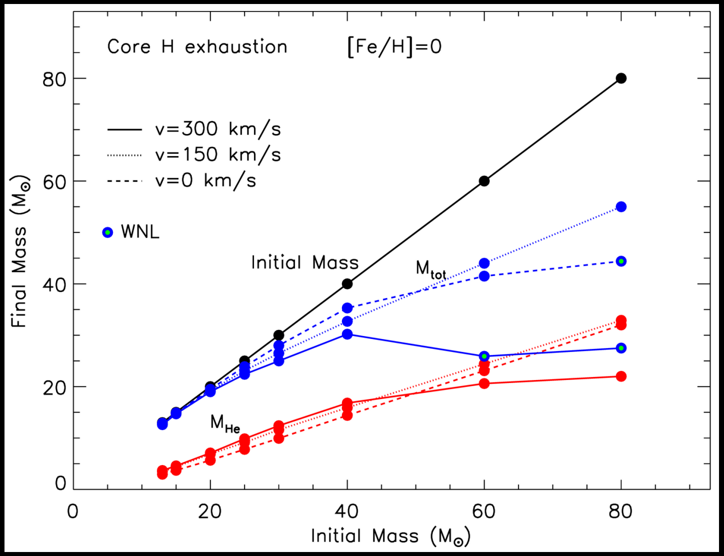

DIRECT EFFECTS

Internal Mixing (meridional circulation, shear diffusion)

- Larger Cores and Longer Evolutionary Times (these effects are negligible after core He depletion due to the dramatic shortening of the advanced evolutionary phases)
- Surface enrichment in elements produced in the innermost zones
- More Compact Structures → Higher Luminosities

Reduction of the Effective Gravity (centrifugal force, angular momentum transport)

- More Expanded Envelopes → Lower Effective Temperatures

Mechanical Mass Loss

- Increase of Mass Loss if the star reaches the Critical Velocity

INDIRECT EFFECTS

Higher Luminosities and Lower Effective Temperatures → Increase of Mass Loss efficiency

Decreasing the metallicity →

- Increase of Rotation Induced Mixing $\tau_{diff} \sim \frac{\Delta R^2}{D}$
- Decrease of Mass Loss efficiency $\dot{M} \sim Z^{0.85}$

He Core Mass @ Core H Depletion

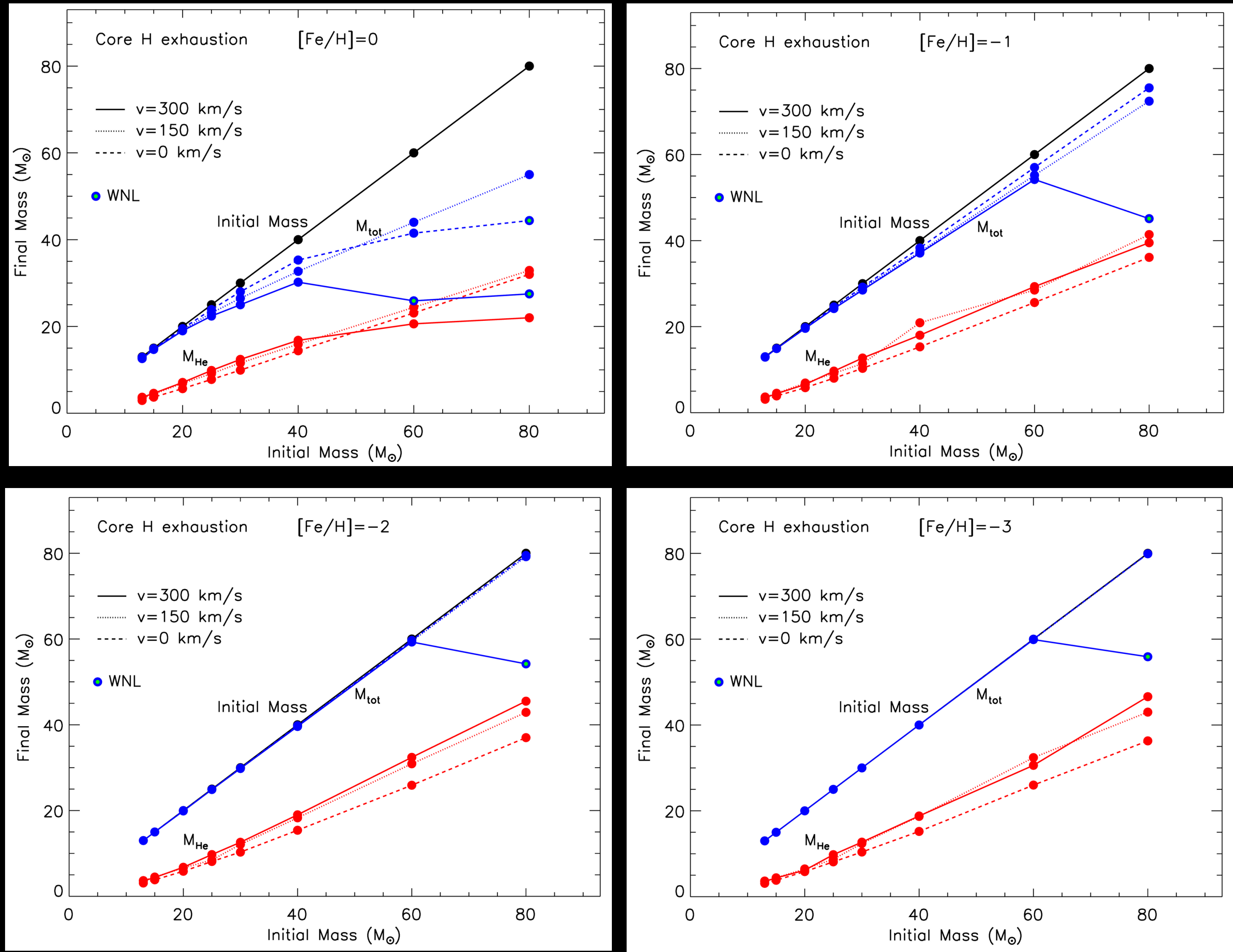

Core He Burning: Solar Metallicity Models

After core H depletion, all the models (except 60 and 80 $M_{\odot}$ v=300 km/s) evolve toward a RSG configuration

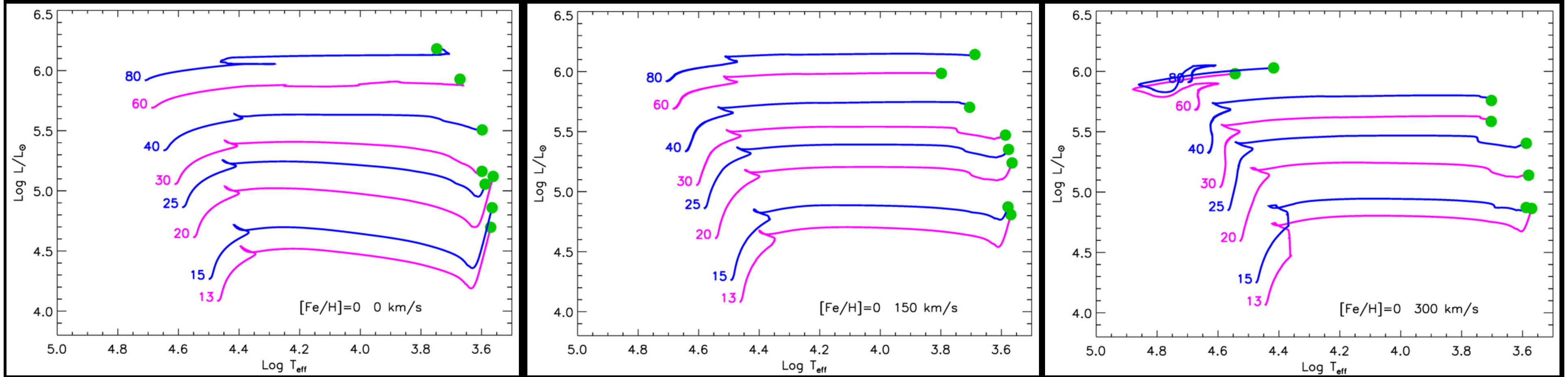

During the following evolution (core He burning)

- The higher mass models may reach the Eddington limit → most of the H-rich envelope is lost and the star evolves to the a BSG configuration
- The lower mass models may become cool enough that dust driven wind becomes very efficient. The central He mass fraction at which this occurs determines how much mass is lost during core He burning and weather the star evolves to a BSG (WR) configuration

Core He Depletion: Solar Metallicity Models

Configuration @ He depletion

Rotating models are more luminous and cooler → Eddington limit and dust production favored

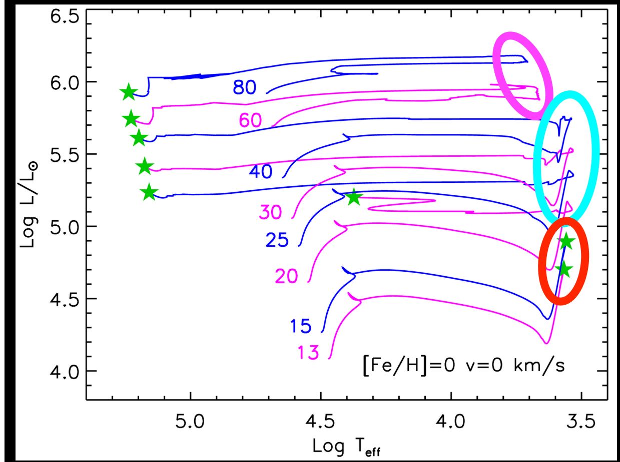

v=0 km/s

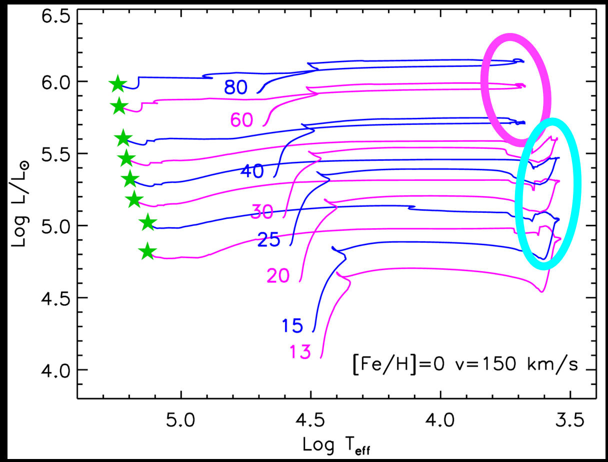

v=150 km/s

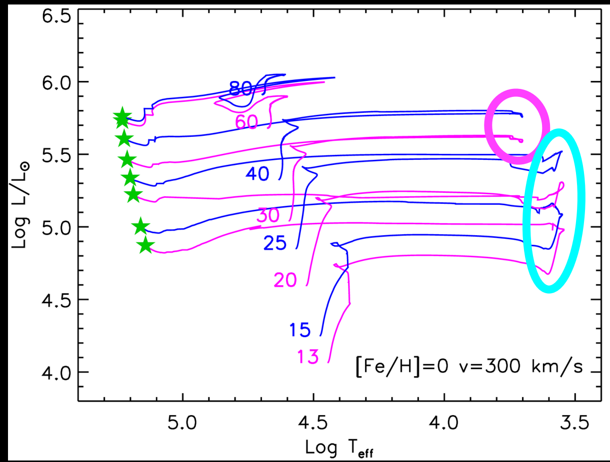

v=300 km/s

Stars that reach the Eddington limit

Stars entering the dust production
in an early stage of core He burning
→ becomes BSG/WR stars

Stars entering the dust production
in a late stage of core He burning
→ remains RSG

Core He Depletion: Solar Metallicity Models

Configuration @ He depletion

v=0 km/s

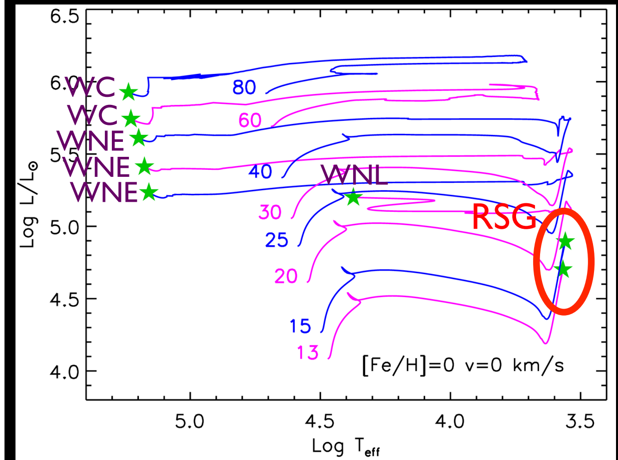

v=150 km/s

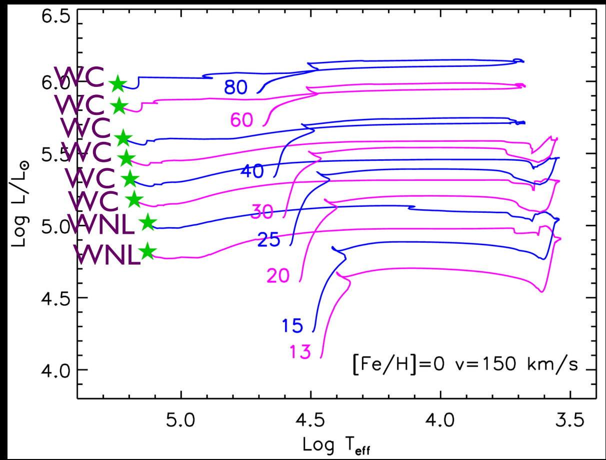

v=300 km/s

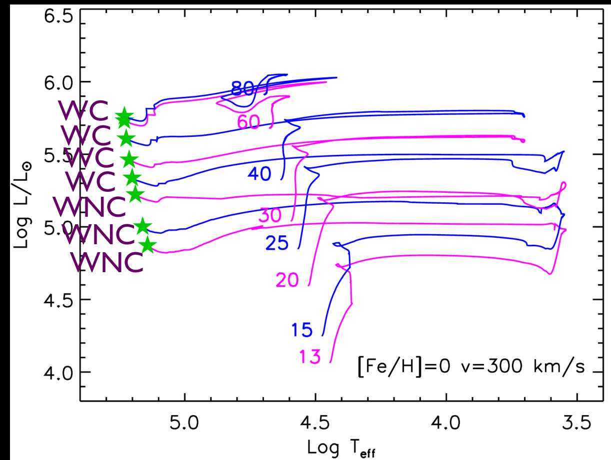

$M \geq 20\ M_\odot$ → WR | $M \geq 13\ M_\odot$ → WR | $M \geq 13\ M_\odot$ → WR

$M \leq 15\ M_\odot$ → RSG

WR : $\mathrm{Log}_{10}(T_{eff}) > 4.0$

- WNL: $10^{-5} < H_{sup} < 0.4$ (H burning, CNO, products)
- WNE: $H_{sup} < 10^{-5}$ (No H)
- WNC: 0.1 < X(C)/X(N) < 10 (both H and He burning products, N and C)
- WC: [X(C)+X(O)]/X(He) < 1 (He burning products)
- WO: [X(C)+X(O)]/X(He) ≥ 1 (He burning products)

INAF

KAVLI IPMU INSTITUTE FOR THE PHYSICS AND MATHEMATICS OF THE UNIVERSE

Core He Depletion: Low Metallicity Models

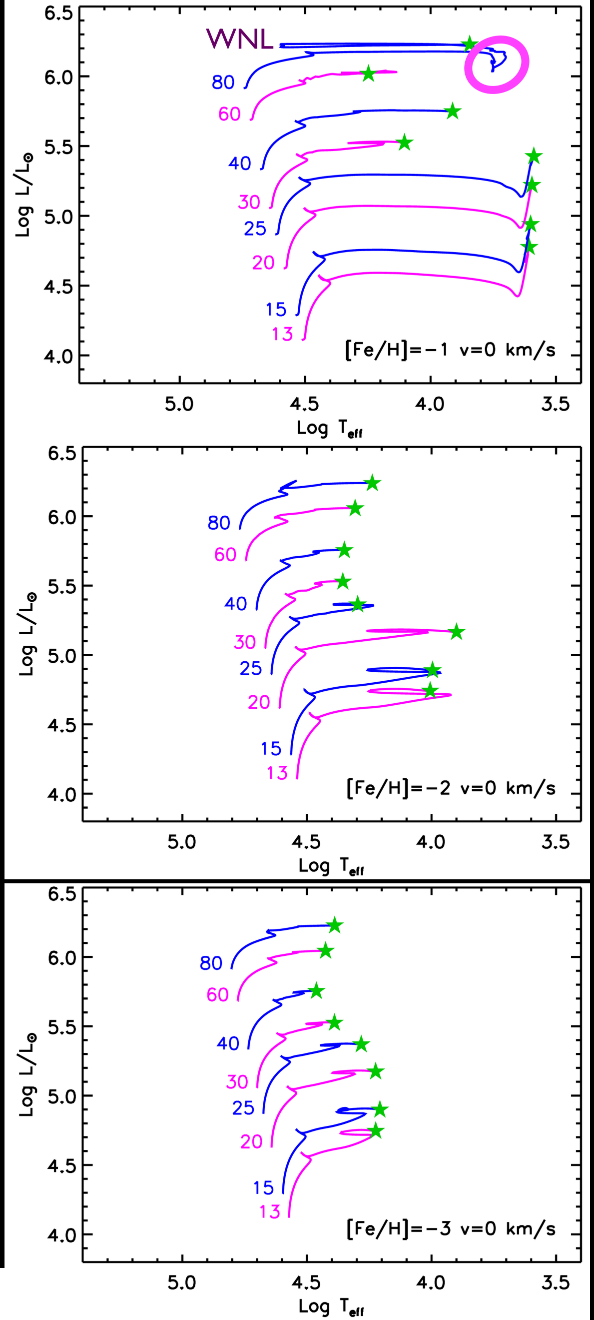

Core He Depletion: Low Metallicity Models

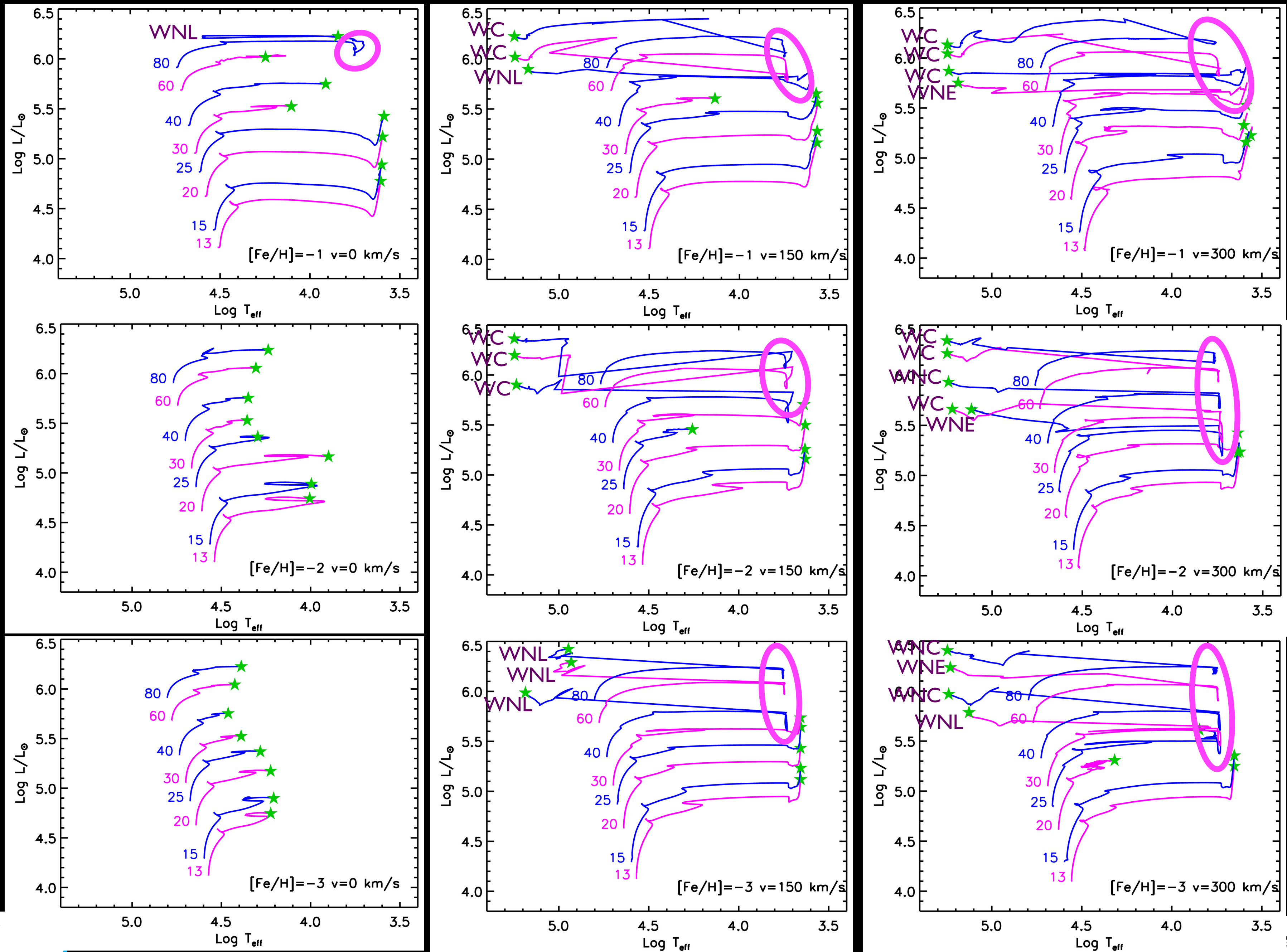

CO Core Mass @ Core He Depletion

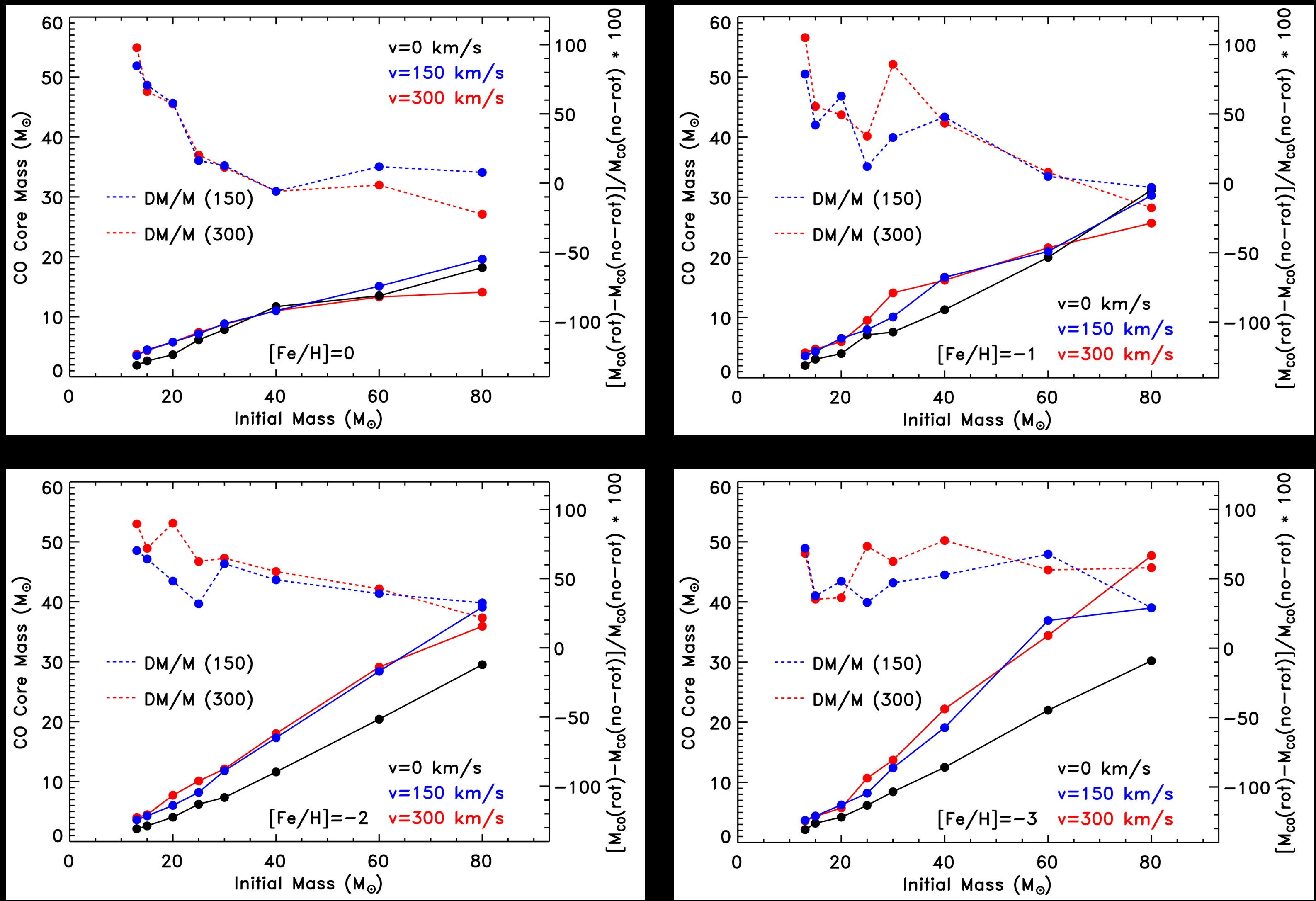

The CO core increases with increasing the initial velocity and with decreasing the metallicity

CO Core Mass @ Core He Depletion

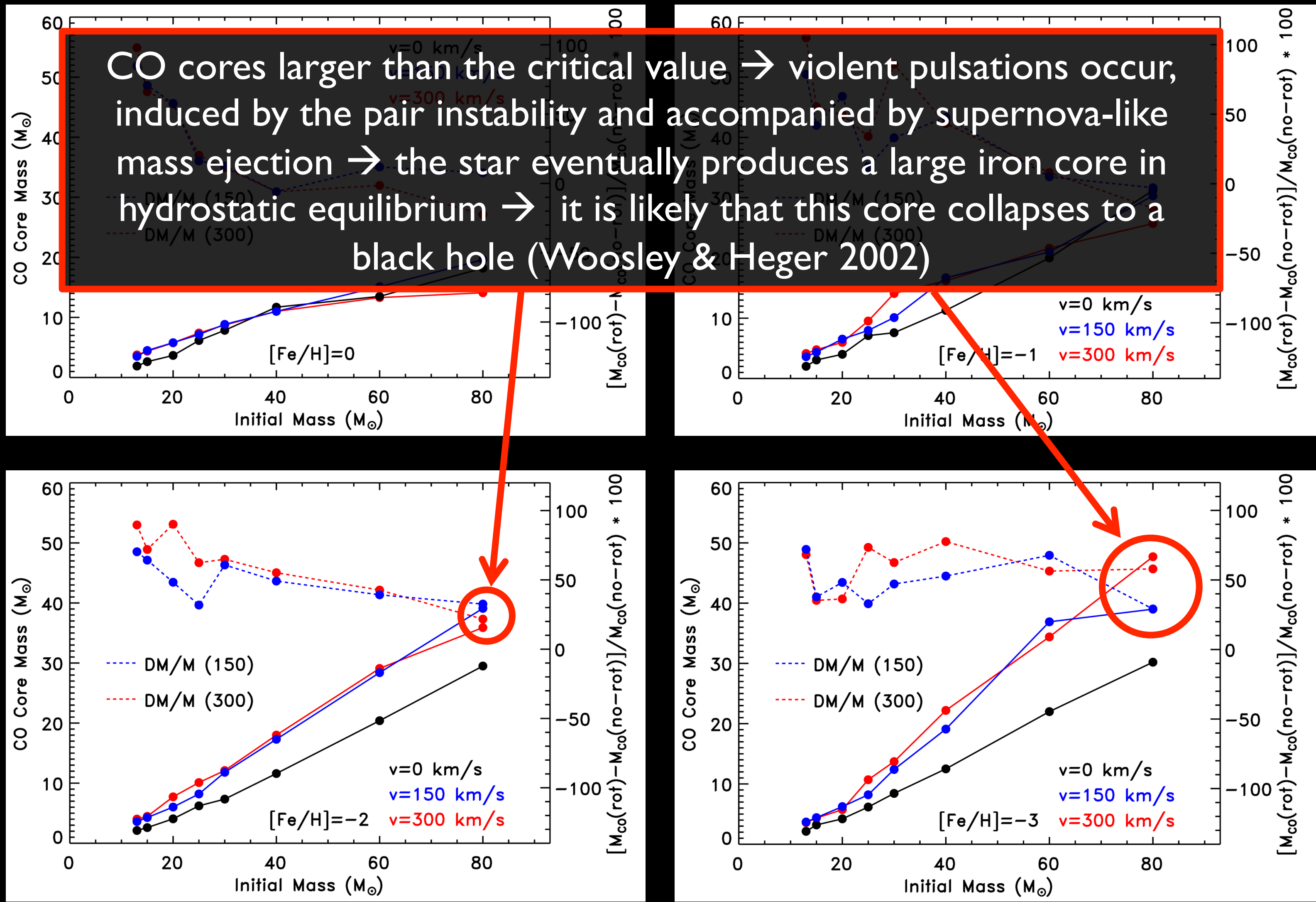

CO cores larger than the critical value → violent pulsations occur, induced by the pair instability and accompanied by supernova-like mass ejection → the star eventually produces a large iron core in hydrostatic equilibrium → it is likely that this core collapses to a black hole (Woosley & Heger 2002)

The CO core increases with increasing the initial velocity and with decreasing the metallicity

Advanced Burning Stages

Larger CO at core He depletion → Stronger contraction of the CO core

Presupernova rotating models (M<40 $M_\odot$) appear much more compact compared to the non rotating ones, with larger Fe cores and larger binding energies

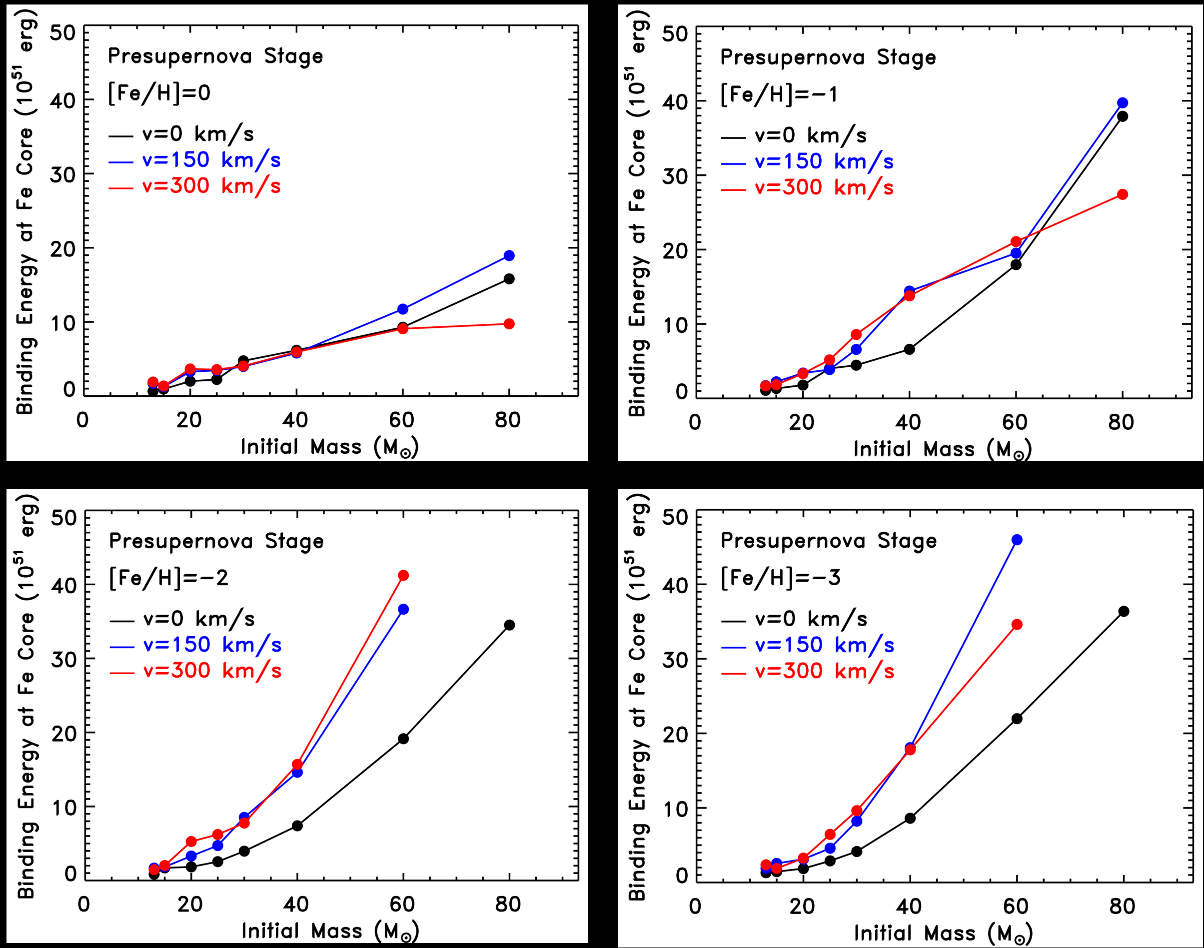

We expect larger remnant masses for lower metallicity rotating models

INAF

KAVLI IPMU INSTITUTE FOR THE PHYSICS AND MATHEMATICS OF THE UNIVERSE

Configuration @ PreSN Stage

Due to the dramatic speed up of the advanced evolutionary stages the location of the star in the HR diagram does not change significantly during these phases

RSG = Red Supergiant (extended) SN Progenitor
BSG = Blue Supergiant (compact) SN Progenitor
WX = Wolf-Rayet (compact) SN Progenitor with no or very little H

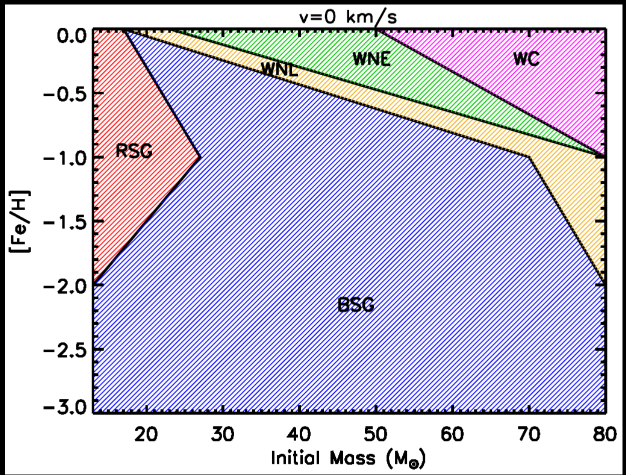

Non Rotating Models: the decrease of Mass Loss with metallicity implies:

- RSG progenitors increase down to [Fe/H]=-1 and then disappears below [Fe/H]=-2
- WR progenitors progressively decrease and disappears below [Fe/H]=-2

Configuration @ PreSN Stage

Due to the dramatic speed up of the advanced evolutionary stages the location of the star in the HR diagram does not change significantly during these phases

RSG = Red Supergiant (extended) SN Progenitor
BSG = Blue Supergiant (compact) SN Progenitor
WX = Wolf-Rayet (compact) SN Progenitor with no or very little H

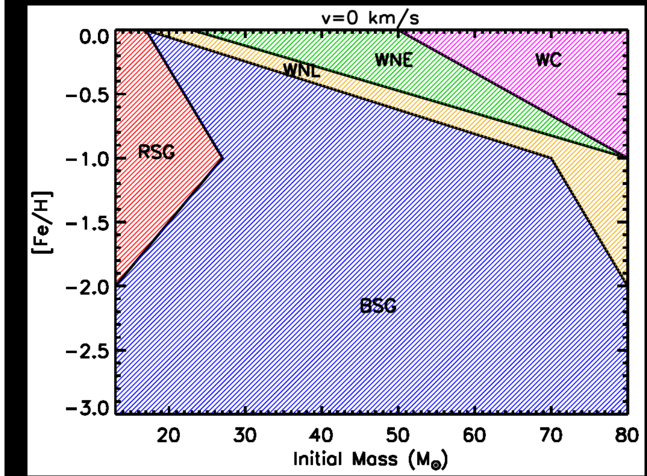

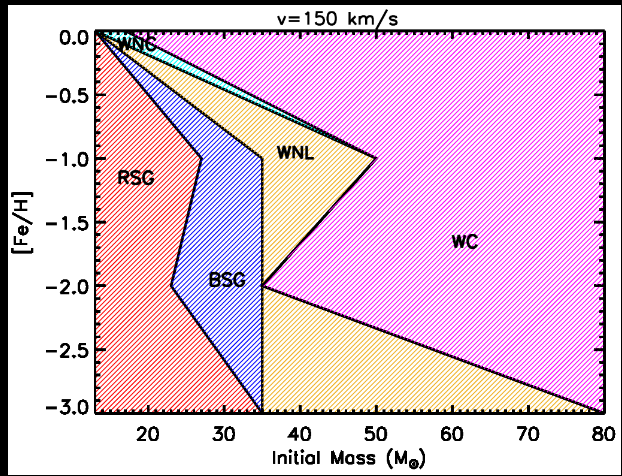

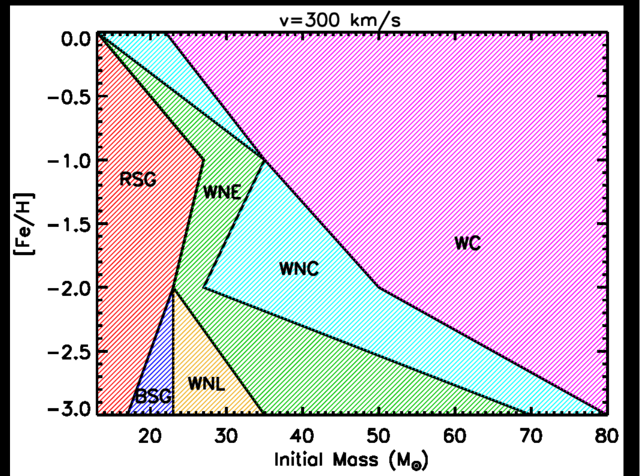

Non Rotating Models: the decrease of Mass Loss with metallicity implies:

- RSG progenitors increase down to [Fe/H]=-1 and then disappears below [Fe/H]=-2
- WR progenitors progressively decrease and disappears below [Fe/H]=-2

Rotating Models: the inclusion of rotation reduces the minimum mass entering the WR phase and increases the maximum mass becoming RSG @ all metallicities

- RSG progenitors increase at lower metallicities (reduction of effective gravity)
- WR progenitors increase at lower metallicities (direct/indirect enhancement of mass loss

The Final Fate: SN Types

Limiting H/He masses for the formation of the various SNe from Hachinger+ 2012

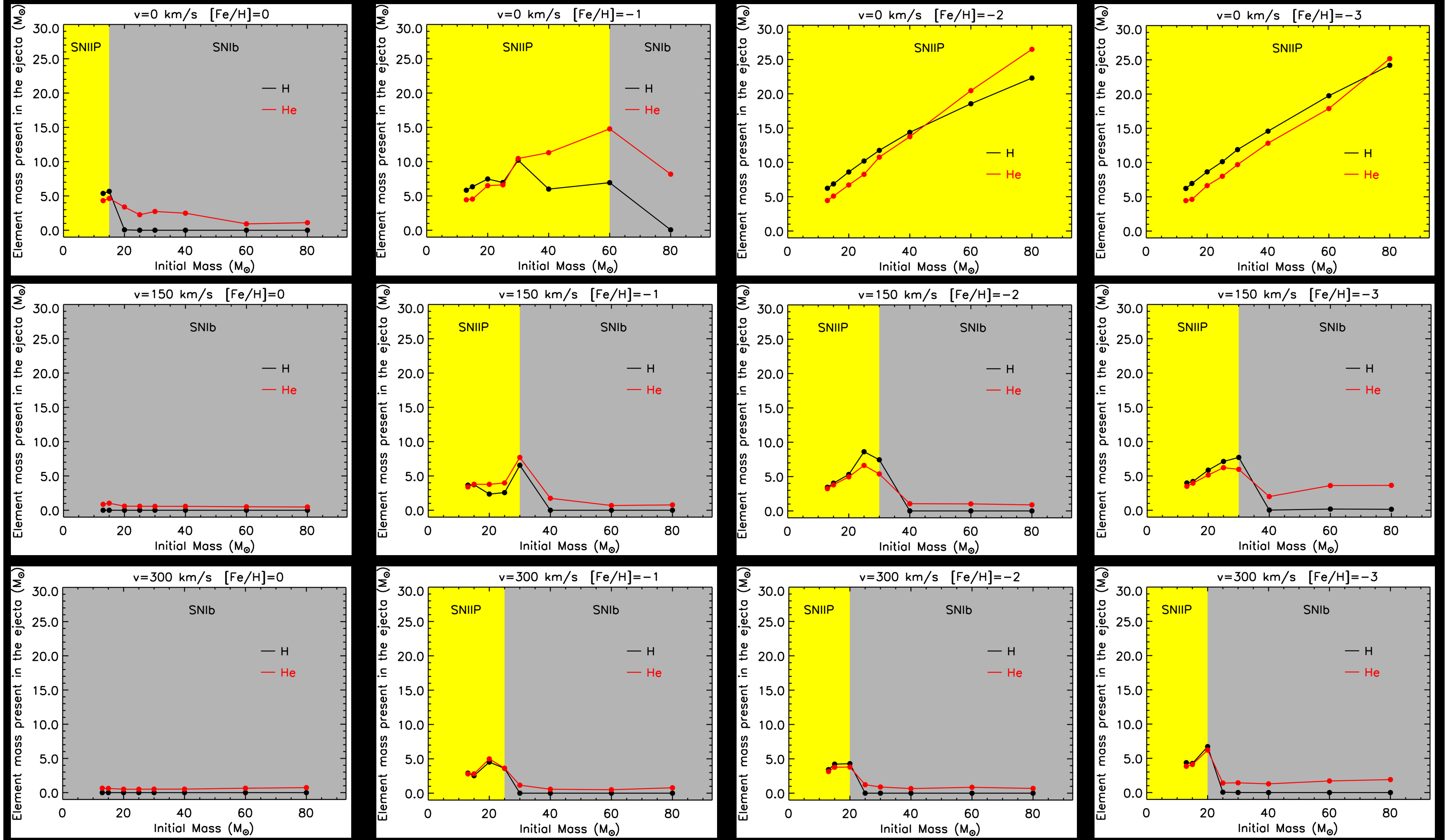

- Increasing fraction of SNIIP with decreasing [Fe/H] and with decreasing v
- No SNIc predicted for any [Fe/H] and v

INDUCED EXPLOSION, EXPLOSIVE NUCLEOSYNTHESIS AND FALLBACK

Propagation of the shock wave followed by means of an explosive simulation code, developed by us, that solves the fully compressible reactive hydrodynamic equations using the piecewise parabolic method (PPM - Colella & Woodward 1984) in the Lagrangean form

Chemical evolution of the matter computed by coupling the same nuclear network adopted in the hydrostatic calculations to the system of hydrodynamic equations.

$$\frac{\partial v}{\partial t} = -\frac{Gm}{r^2} - 4\pi r^2 \frac{\partial P}{\partial m}$$

$$\frac{\partial r}{\partial m} = \frac{1}{4\pi r^2 \rho}$$

$$\frac{\partial e}{\partial t} = \frac{P}{\rho^2}\frac{\partial \rho}{\partial t}$$

$$\frac{\partial Y_i}{\partial t} = \sum_j c_i(j)\lambda_j Y_j + \sum_{j,k} c_i(j,k)\rho N_{\mathrm{A}} < \sigma v >_{j,k} Y_j Y_k + \sum_{j,k,l} c_i(j,k,l)\rho^2 N_{\mathrm{A}}^2 < \sigma v >_{j,k,l} Y_j Y_k Y_l \qquad i = 1, ..., N$$

Chemical Yields @ Various Metallicities and Initial Velocities

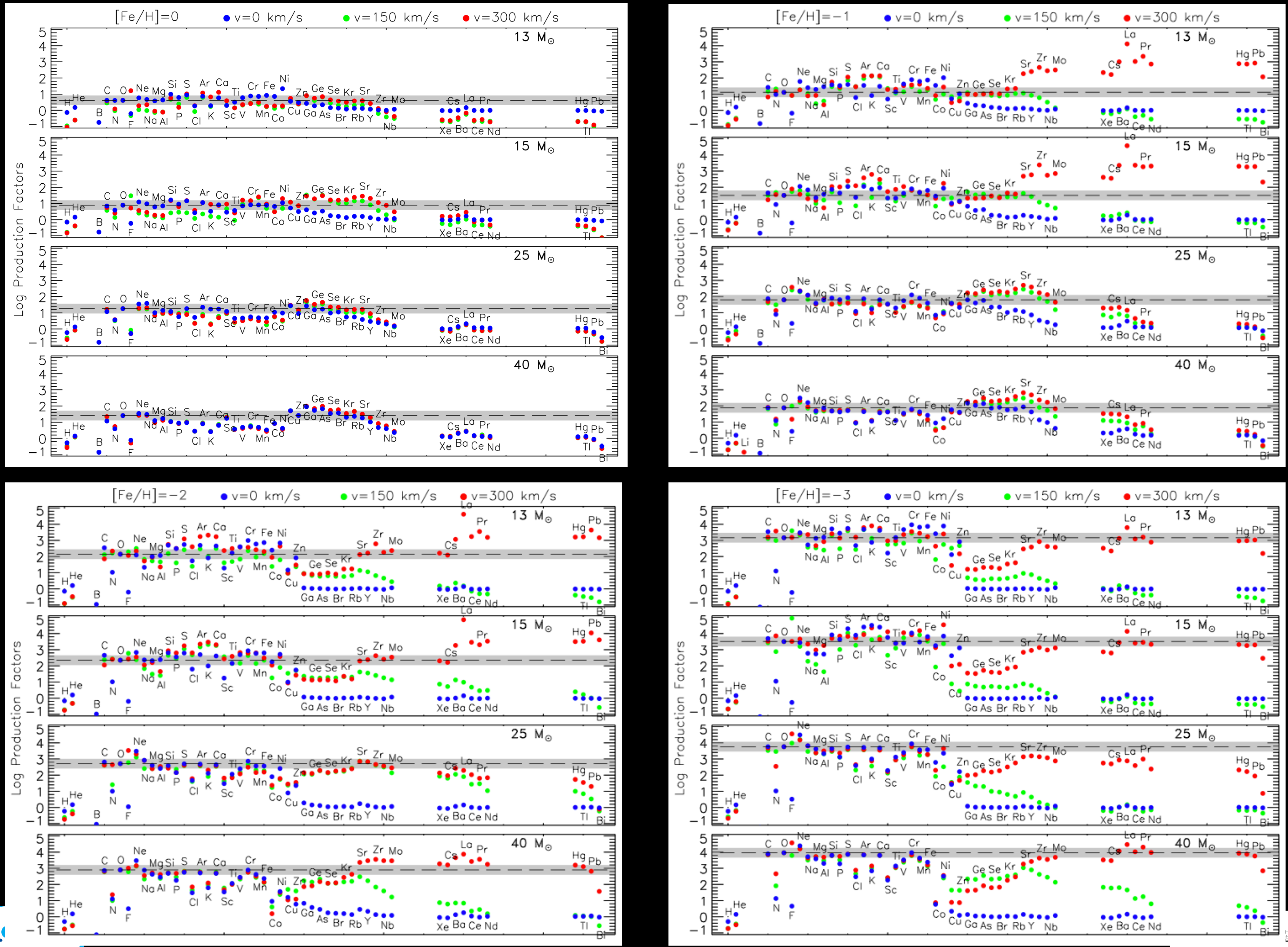

The α-elements O Mg Si Ca: Non Rotating Models

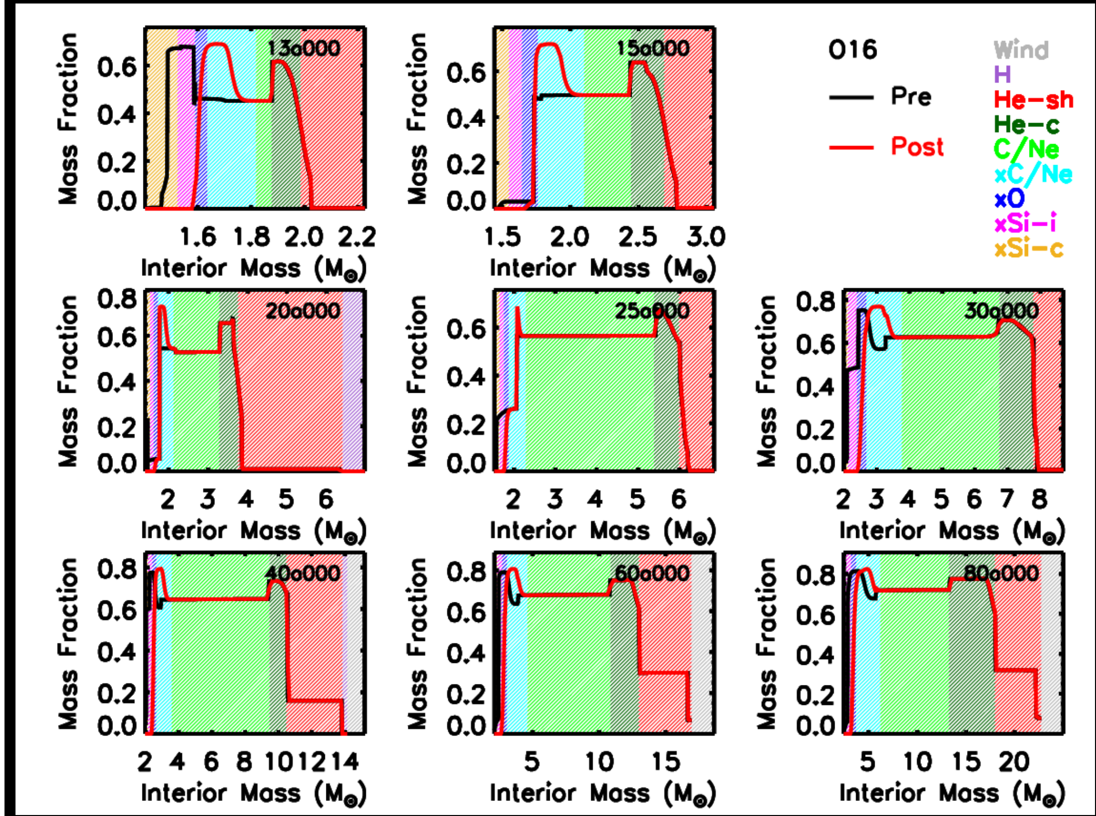

Most abundant isotope: ^{16}O

Production Site: Hydrostatic He burning

N.B. In the less massive stars the hydrostatic production is partially modified by the explosion

Although ^{16}O maybe considered as a "hydrostatic" isotope a reliable value of its yield requires the computation of the explosive nucleosynthesis

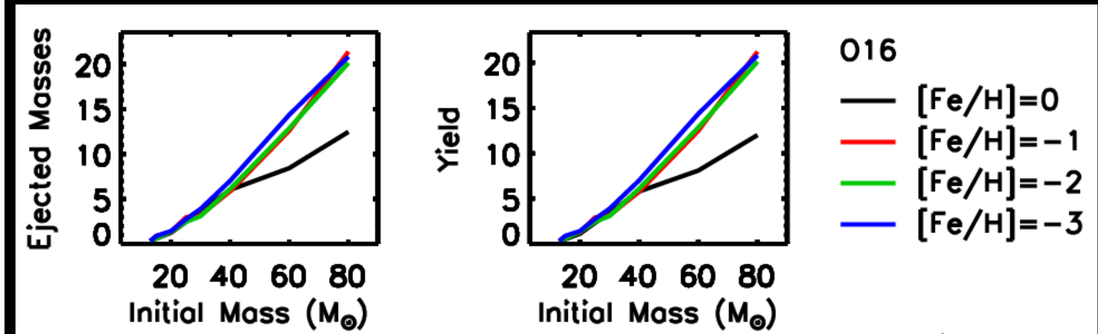

Produced by massive stars

Follows the same trend of the He Core Mass vs Initial Mass

Mild dependence on metallicity with the exception of the most massive solar metallicity stars (mass loss reduces the He core)

The α-elements O Mg Si Ca: Non Rotating Models

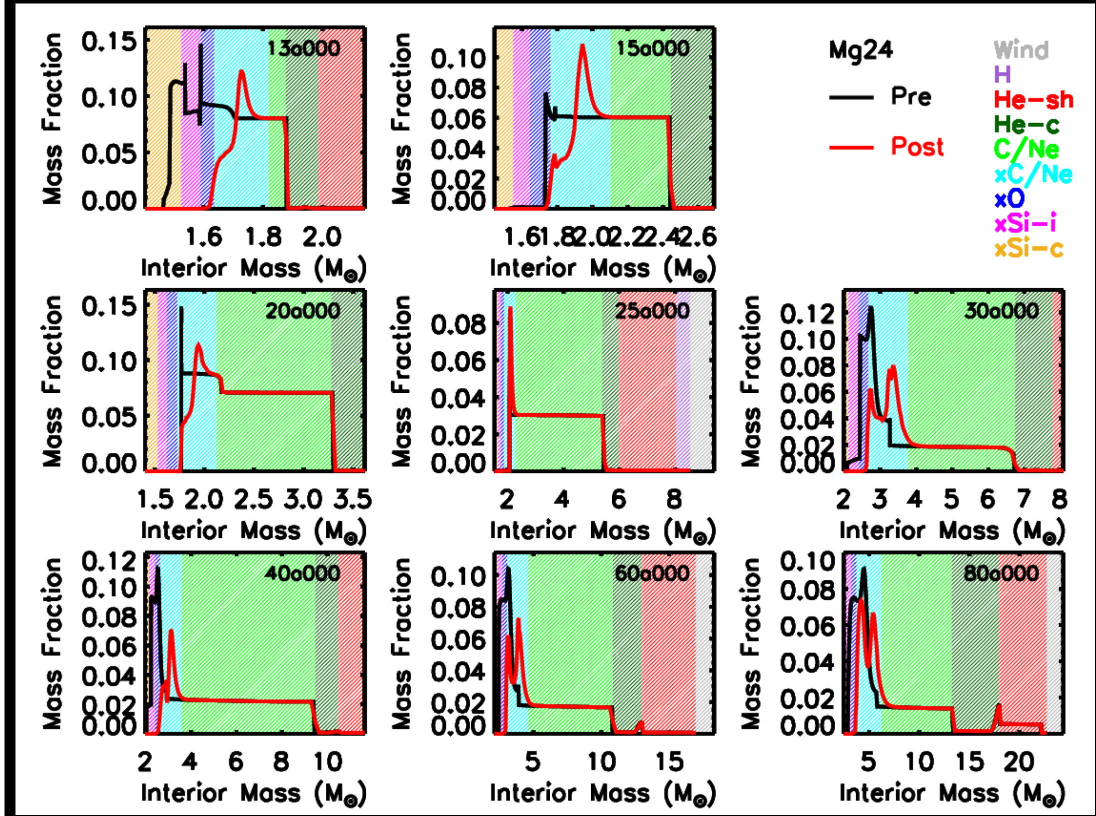

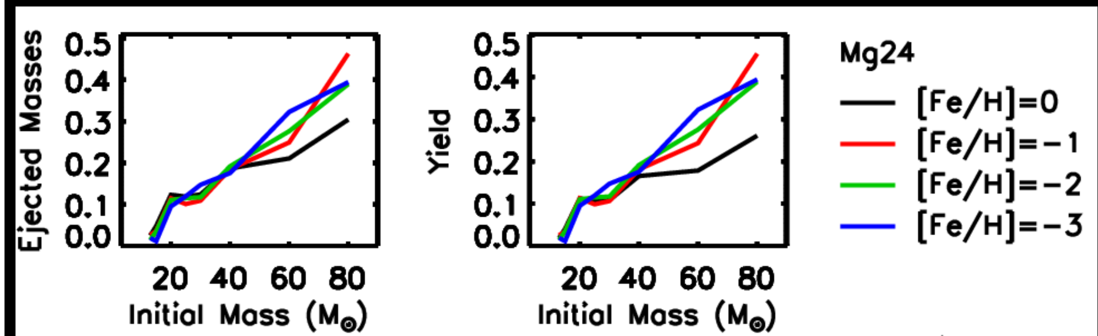

Most abundant isotope: ^{24}Mg

Production Site: Hydrostatic C/Ne burn.

N.B. In the less massive stars the hydrostatic production is even substantially modified by the explosion

Although ^{24}Mg maybe considered as a "hydrostatic" isotope a reliable value of its yield requires the computation of the explosive nucleosynthesis

Produced by massive stars

Follows the same trend of the C/Ne shell Mass vs Initial Mass

Non monothonic dependence on metallicity increasing for massive stars ($M \geq 40\ M_\odot$)

The α-elements O Mg Si Ca: Non Rotating Models

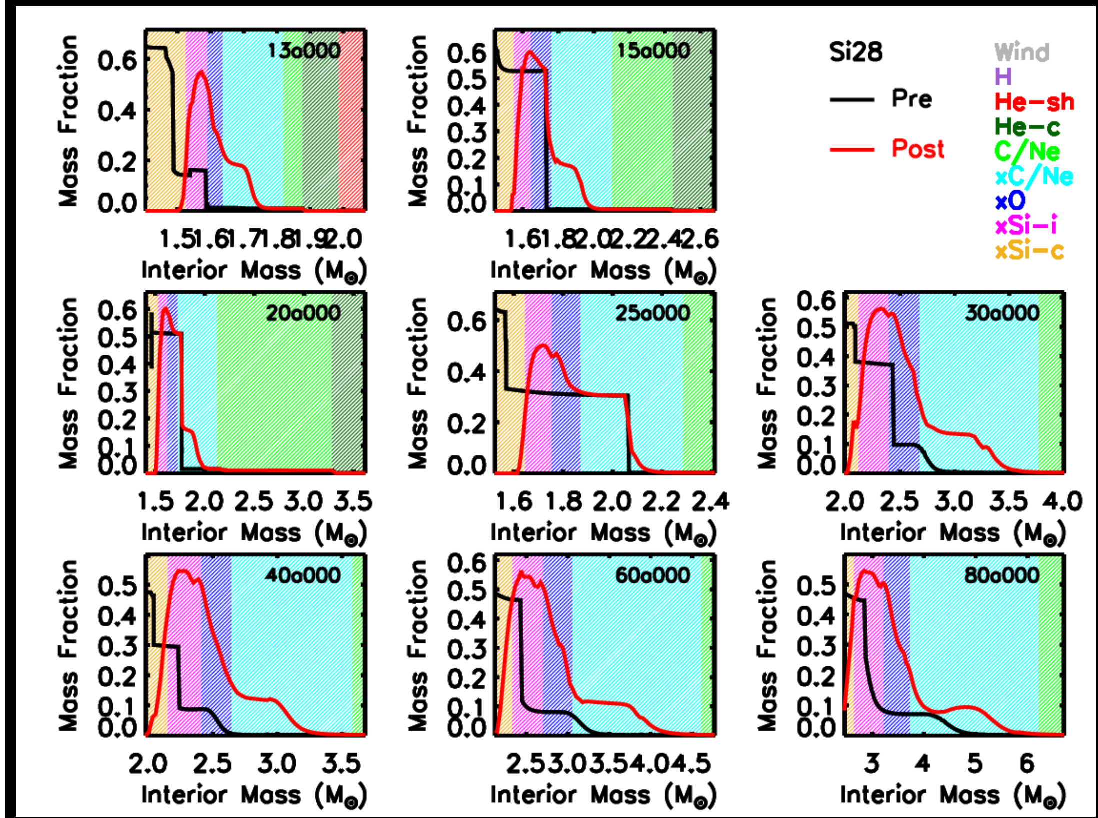

Most abundant isotope: ^{28}Si

Production Site: Hyd. O – Expl. Si-i – Expl. O – Expl. C/Ne

N.B. The relative proportions vary from star to star

The computation of the yield of ^{28}Si necessarily requires the computation of the explosive nucleosynthesis

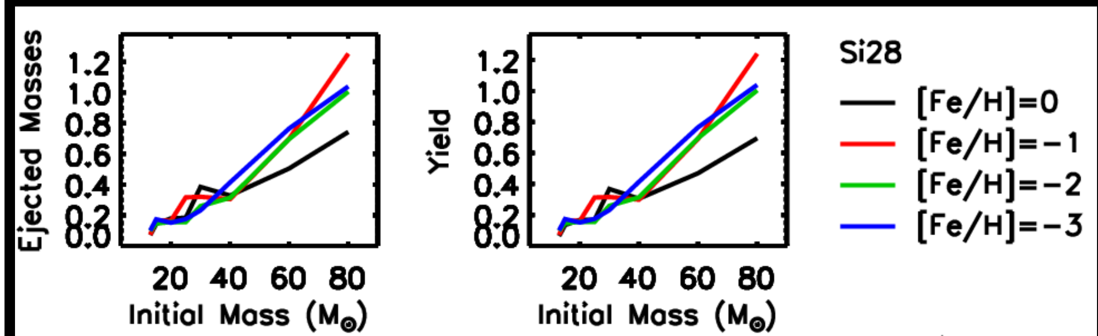

Produced by massive stars

Increases with the initial mass (on average)

Non monothonic dependence on metallicity. Larger variations for the most massive stars (M≥40 M$_\odot$)

The α-elements O Mg Si Ca: Non Rotating Models

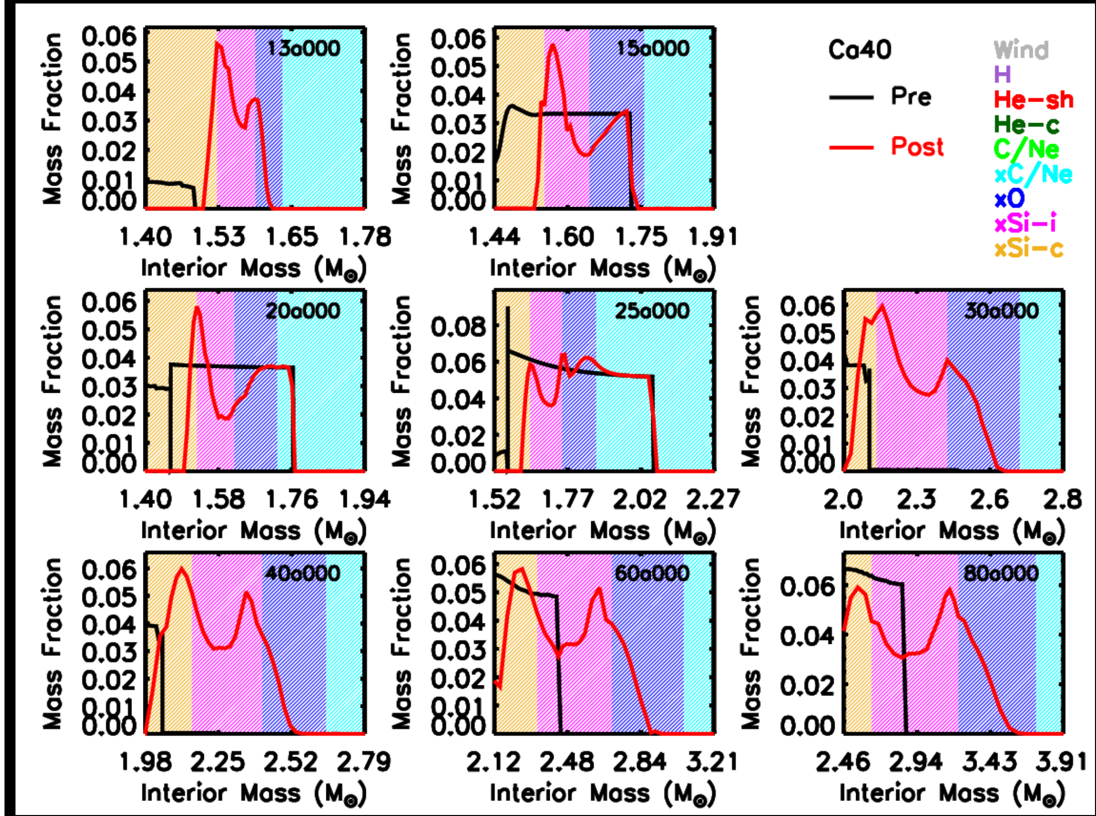

Most abundant isotope: ^{40}Ca

Production Site: Hyd. O – Expl. Si-C – Expl. Si-i – Expl. O

N.B. The relative proportions vary from star to star

The computation of the yield of ^{40}Ca necessarily requires the computation of the explosive nucleosynthesis

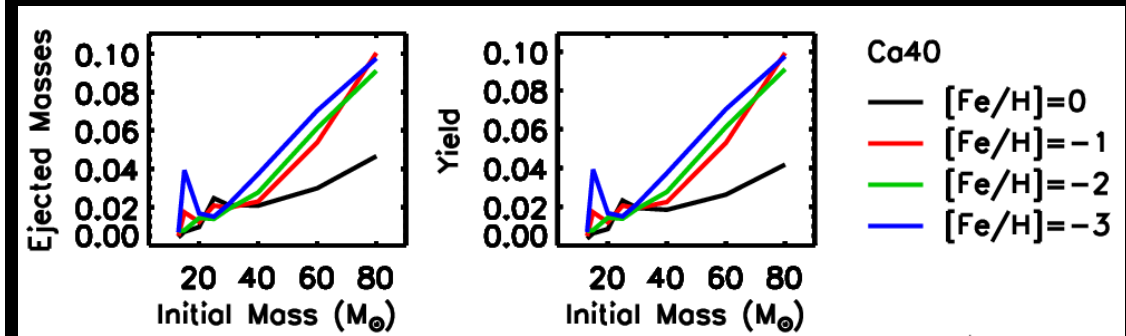

Produced by massive stars

On average it increases with the mass and decreases with the metallicity although the behavior is not always monothonic

The α-elements O Mg Si Ca: Non Rotating Models

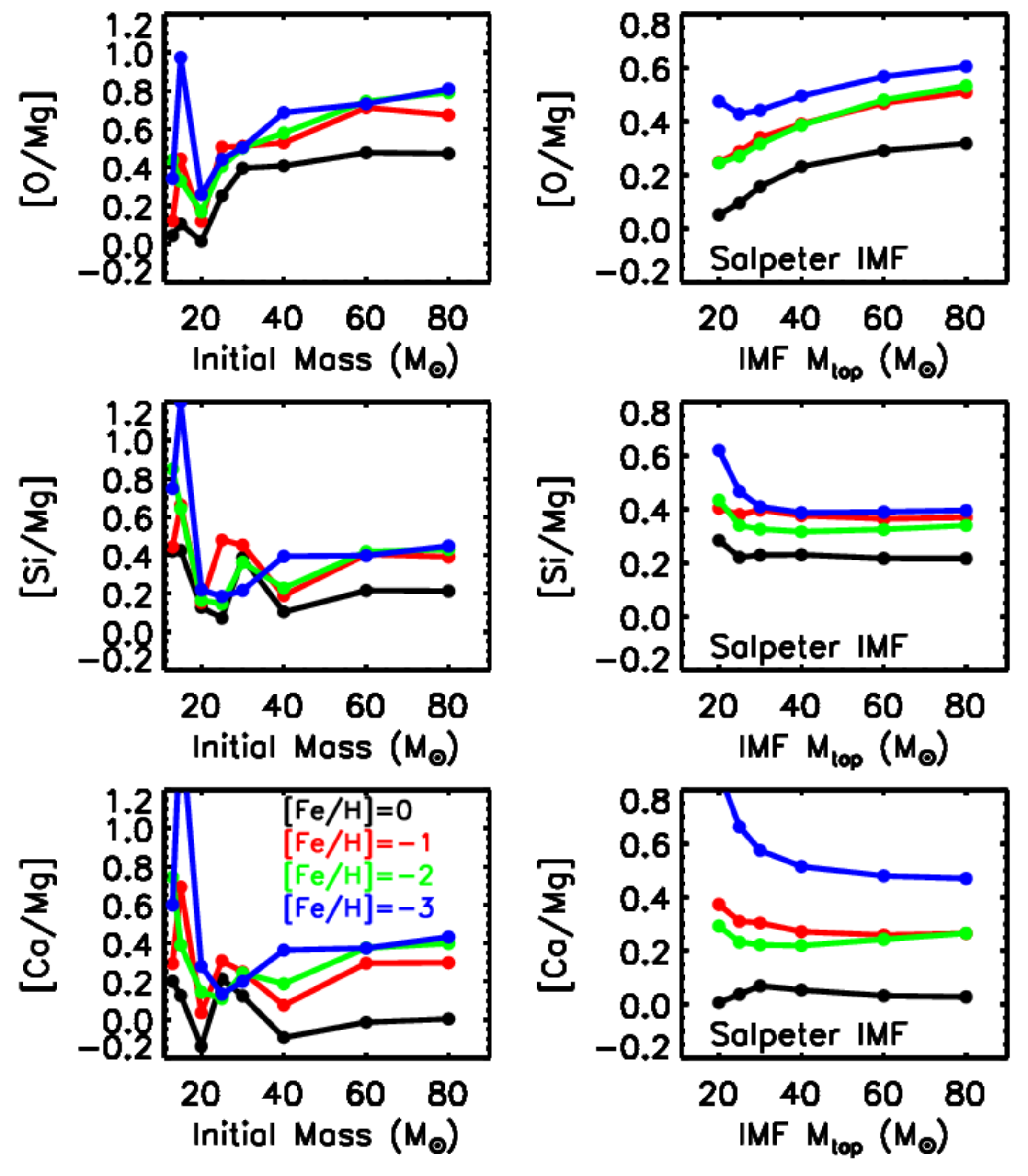

Increases on average with the mass and decreases with the increasing the metallicity

The most massive stars play a role

Decrease on average with the mass up to M~40 $M_\odot$. For higher masses they are almost constant.
They decrease with the increasing the metallicity

The most massive stars does not change substantially [Si,Ca/Mg]

INAF

Kavli IPMU Institute for the Physics and Mathematics of the Universe

The α-elements O Mg Si Ca: Non Rotating Models

Comparison with Woosley & Weaver 1995 (WW95)

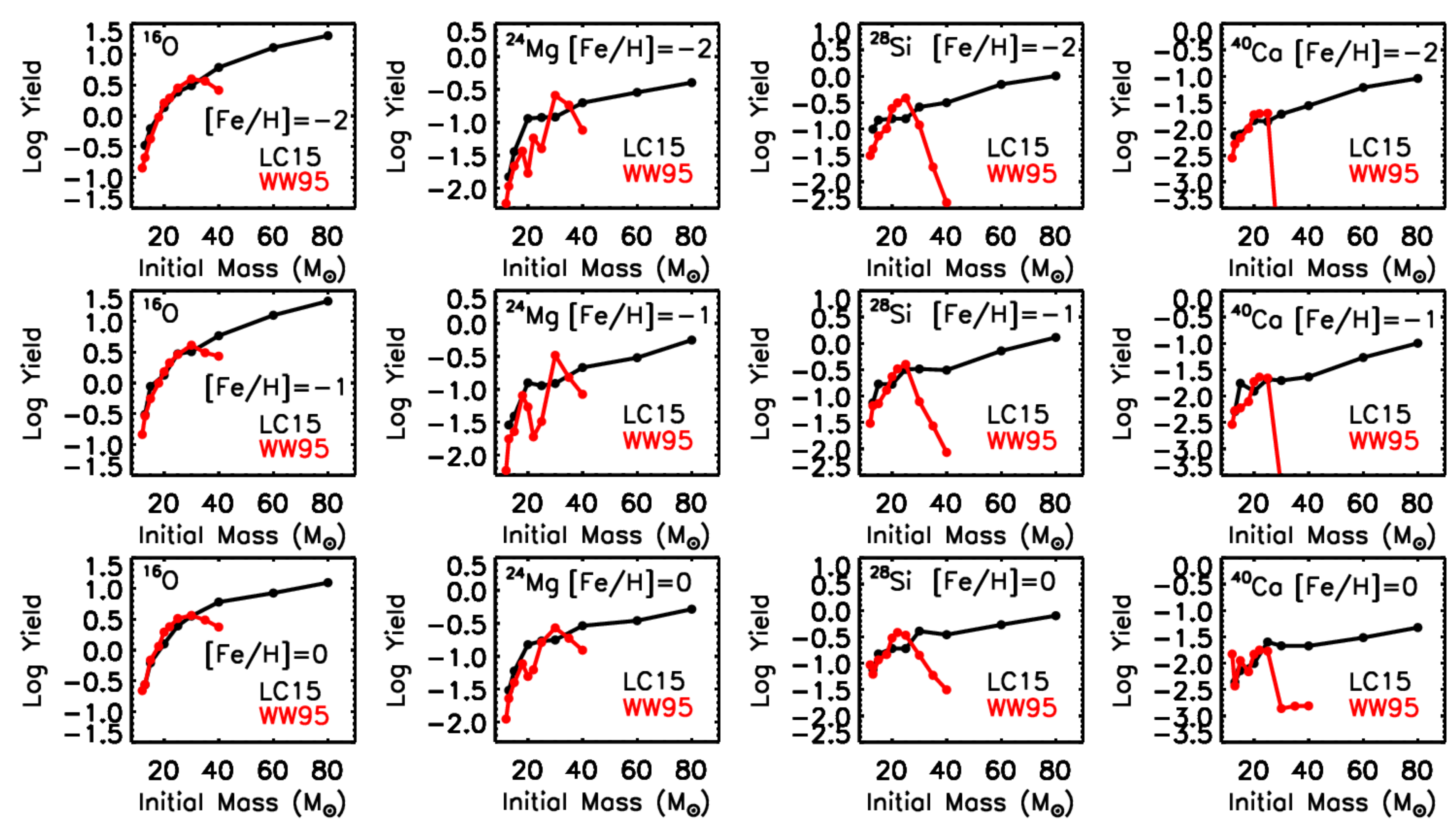

The α-elements O Mg Si Ca: Non Rotating Models

Comparison with Woosley & Weaver 1995 (WW95)

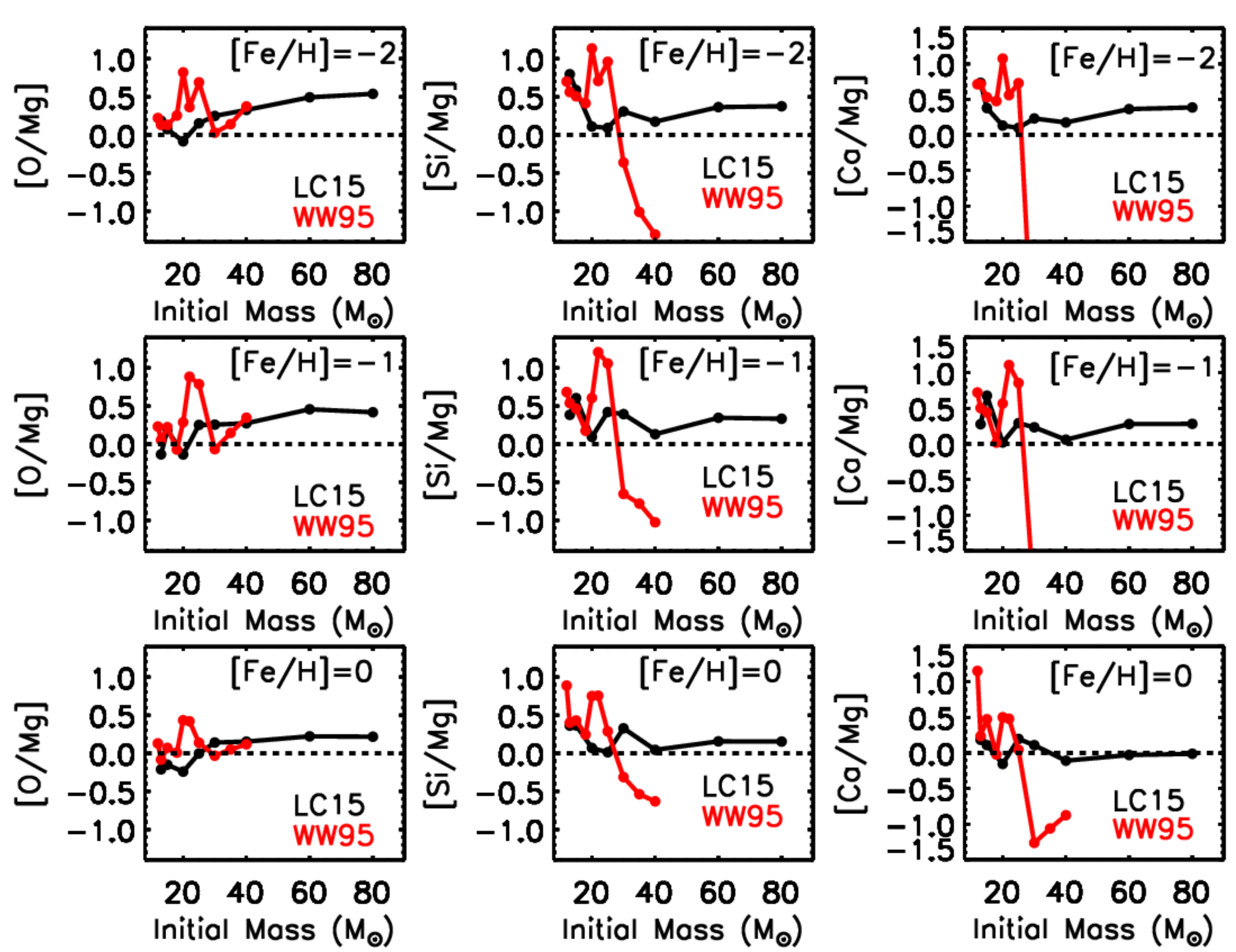

The α-elements O Mg Si Ca: Non Rotating Models

Comparison with Woosley & Weaver 1995 (WW95)

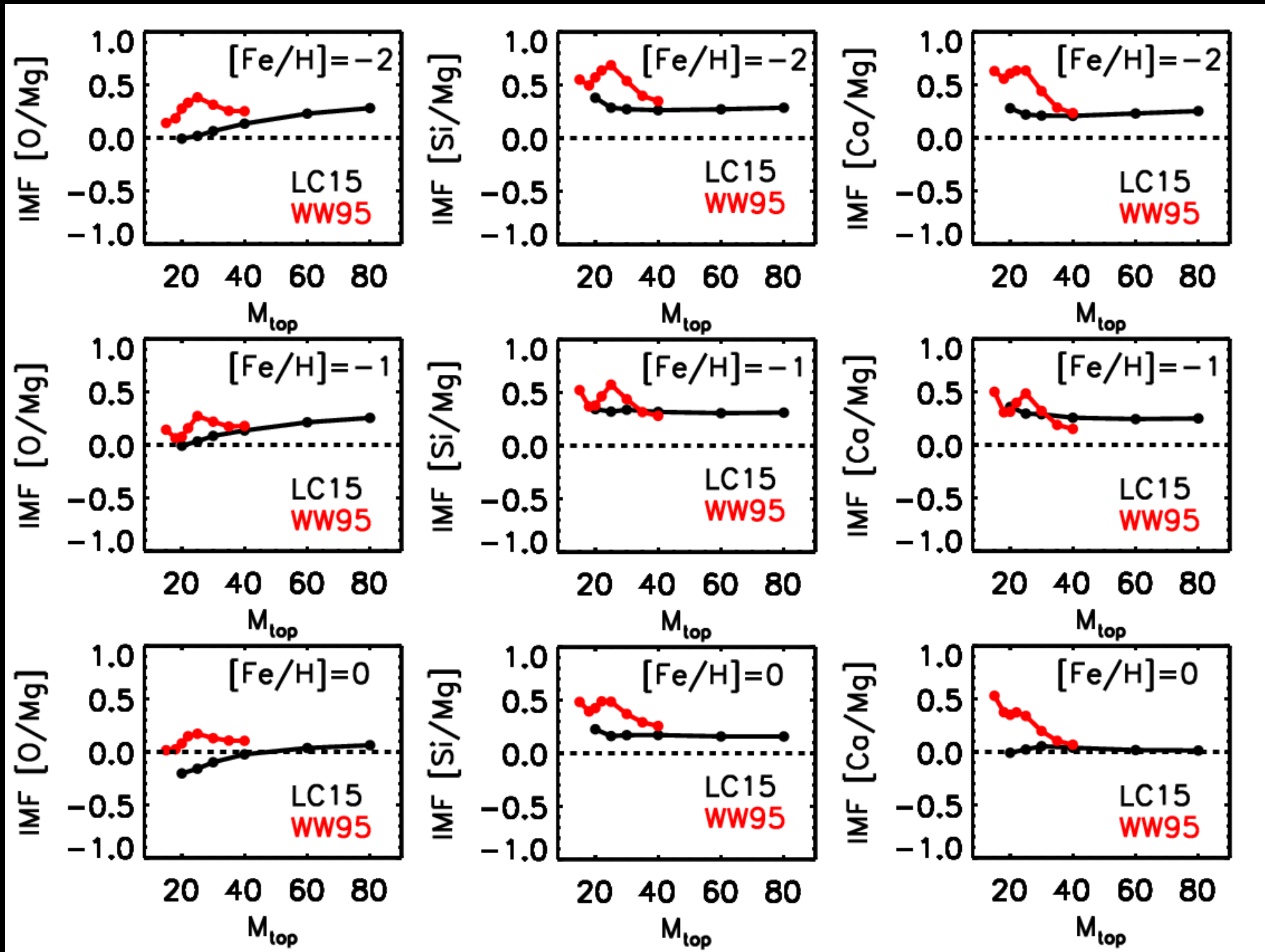

The α-elements O Mg Si Ca: Effect of Rotation

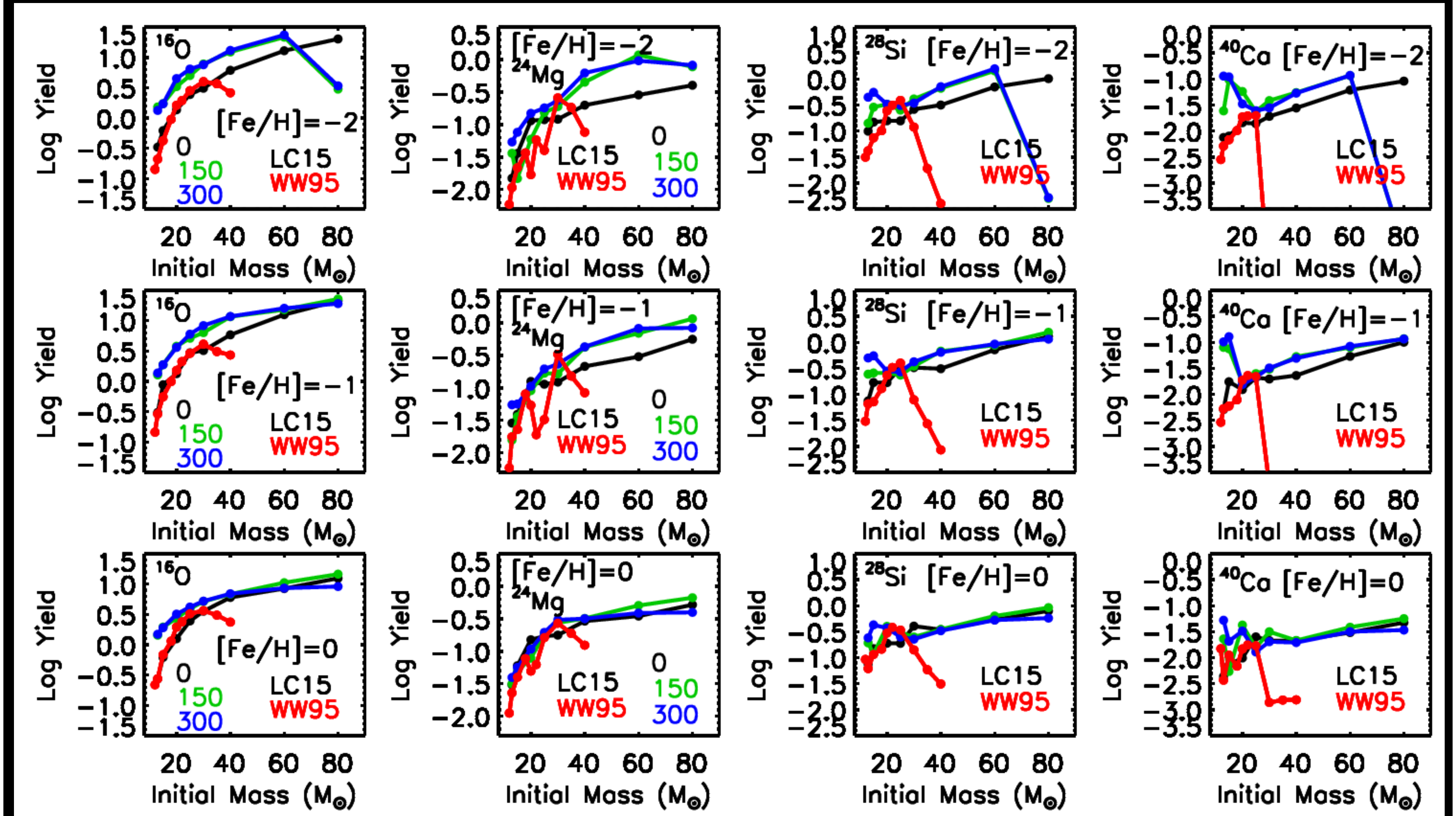

The α-elements O Mg Si Ca: Effect of Rotation

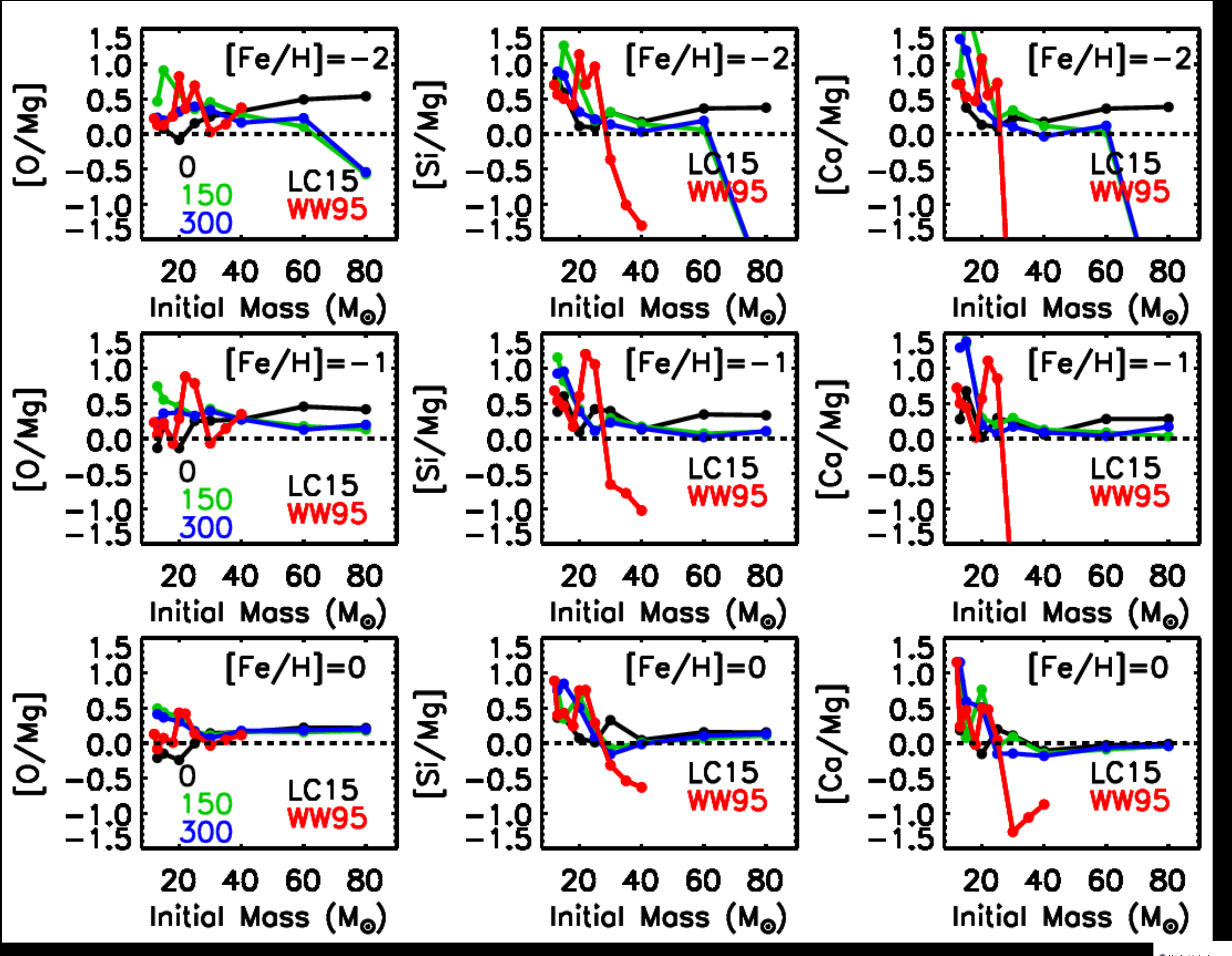

The α-elements O Mg Si Ca: Effect of Rotation

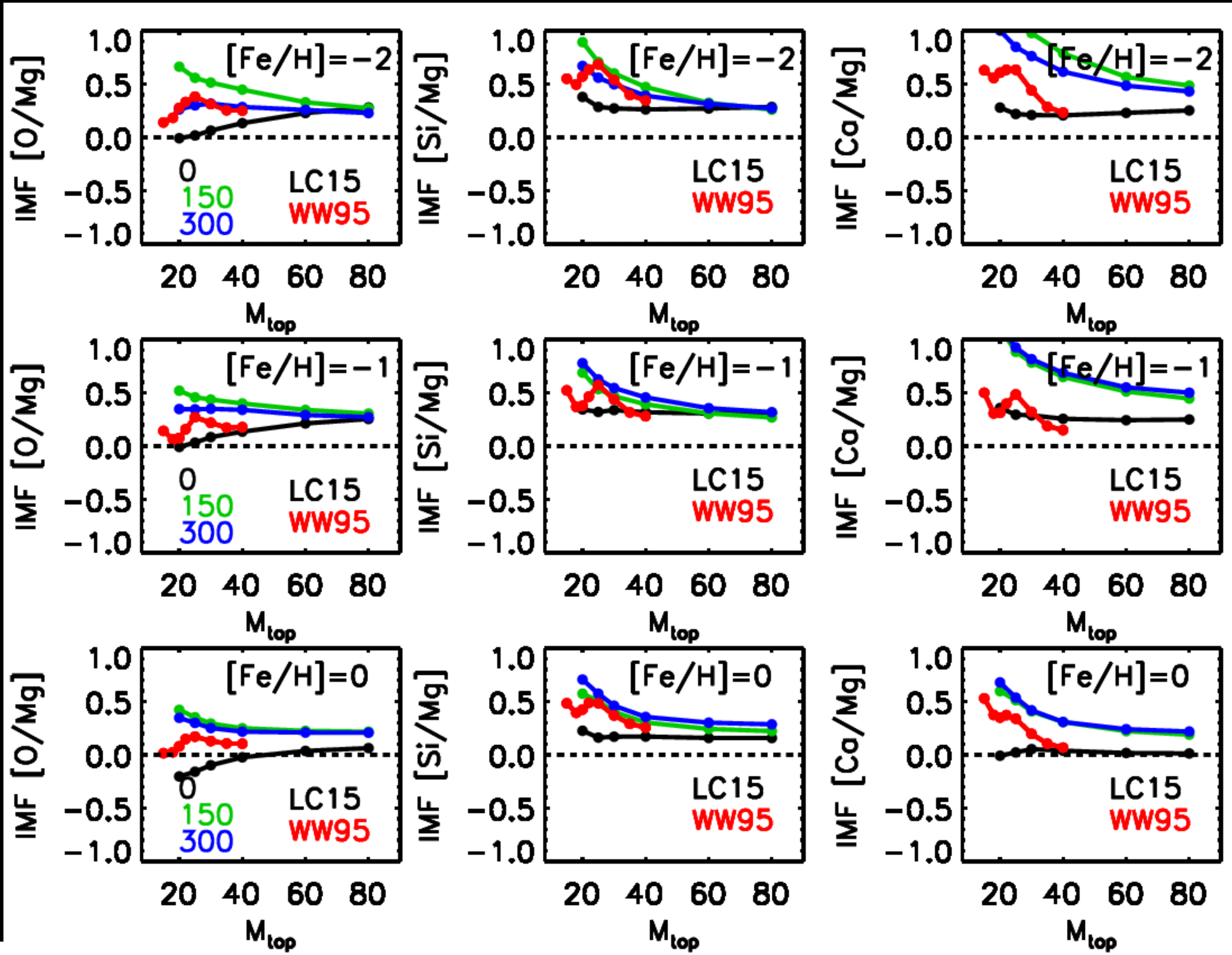

Summary and Conclusions

The inclusion of rotation makes:

- Larger cores (direct effect)
- More efficient mass loss (indirect effect)

The inteprlay between these two effects lead to:

- More compact structure @ preSN stage → more massive remnants
- Increase of the RSG and WR SN progenitors at all metallicities
- Increase of SNIb/SNII fraction at all metallicities

Nucleosynthesis:

- PFs of the majority of the elements increase with the mass for any fixed metallicity and increase for any fixed mass with decreasing the metallicity
- No production of elements heayer than Zn is obtained in non rotating models for metallicities [Fe/H]<-1
- The inclusion of rotation enhances the production of N, F and all the elements heavier than Zn up to Pb
- This effect is higher for lower metallicities (more efficient rotational mixing) and for lower mass models (higher angular momentum for a fixed initial velocity)

Summary and Conclusions

[O/Mg], [Si/Mg] and [Ca/Mg] we find:

For non rotating models:

- [O/Mg] decreases with the mass while [Si,Ca/Mg] increase with the mass
- All of them decrease with decreasing the metallicity
- Same behavior is found for the ratios integrated over a IMF
- The inclusion of more massive stars (M>40 $M_\odot$) lead to an increase of the IMF integrated [O/Mg] by about 0.1-0.2 dex. No sizeable variation is found for [Si,Ca/Mg]
- WW95 ^{16}O, ^{28}Si and ^{40}Ca yields are on average lower for lower masses (M 20 $M_\odot$) ad larger for larger masses at all metallicities. WW95 models of mass (M>40 $M_\odot$) do not ejected substanital amounts of heavy elements
- WW95 ^{24}Mg is always lower than ours at all metallicities
- A similar behavior is found for the individual ratios
- Our ratios integrated over a IMF up to M=40 $M_\odot$ are always lower than the corresponding WW95 values (~0.1 dex) or in some cases in agreement
- Integration up to 80 $M_\odot$ lead to similar results for the two sets of yields

Summary and Conclusions

[O/Mg], [Si/Mg] and [Ca/Mg] we find:

For rotating models:

- The ejected masses of all these element tend to increase because of the increase of the He core mass due to rotational mixing. This effect being different from star to star
- All these ratios are larger for lower mass models and lower for higher mass models . For [Fe/H]=0 negligible effect for the most massive stars
- No difference for the integrated [O/Mg] and [Si/Mg] at [Fe/H]=2, -1. Increase of 0.1-0.2 dex at [Fe/H]=0 compared to non rotating models
- Increase of integrated [Ca/Mg] by 0.2-0.3 dex compared to non rotating models at all metallicities